Bel Hadj Ali, N., Rhode-Barbarigos, L. and Smith, I.F.C. "Analysis of clustered tensegrity structures using a modified dynamic relaxation algorithm" International Journal of Solids and Structures, Vol. 48, No. 5, 2011, pp 637-64. doi:10.1016/j.ijsolstr.2010.10.029

Analysis of clustered tensegrity structures using a modified dynamic relaxation algorithm

Nizar Bel Hadj Ali*, Landolf Rhode-Barbarigos and Ian F.C. Smith

Applied Computing and Mechanics Laboratory
Ecole Polytechnique Fédérale de Lausanne (EPFL)
ENAC/IIC/IMAC, Station 18, 1015 Lausanne, Switzerland

Structure of the paper

Abstract

Tensegrities are spatial, reticulated and lightweight structures that are increasingly investigated as structural solutions for active and deployable structures. Tensegrity systems are composed only of axially loaded elements and this provides opportunities for actuation and deployment through changing element lengths. In cable-based actuation strategies, the deficiency of having to control too many cable elements can be overcome by connecting several cables. However, clustering active cables significantly changes the mechanics of classical tensegrity structures. Challenges emerge for structural analysis, control and actuation. In this paper, a modified dynamic relaxation (DR) algorithm is presented for static analysis and form-finding. The method is extended to accommodate clustered tensegrity structures. The applicability of the modified DR to this type of structure is demonstrated. Furthermore, the performance of the proposed method is compared with that of a transient stiffness method. Results obtained from two numerical examples show that the values predicted by the DR method are in a good agreement with those generated by the transient stiffness method. Finally it is shown that the DR method scales up to larger structures more efficiently.

Keywords: Dynamic Relaxation, Tensegrity Structures, Clustered Actuation, Active Control, Deployable Structures.

1. Introduction

Recent advances in theory and practice of active structural control have modified the general perception of structures. Upon integration of active elements, structures become dynamic objects capable of interacting with their environments. Increasingly, the ability to adapt to performance demands and environmental conditions has become key design criteria for a range of structural and mechanical systems. Among many structural topologies, the tensegrity concept is one of the most promising for actively controlled structures [1-6]. Tensegrities are spatial, reticulated and lightweight structures that are composed of struts and cables. Stability is provided by the self-stress state in tensioned and compressed elements [7, 8]. The tensegrity concept has applications in fields such as sculpture, architecture, aerospace engineering, civil engineering, marine engineering and biology [9]. Tensegrity structures have a high strength-to-mass ratio and this leads to strong and lightweight structural designs [10-12]. Furthermore, tensegrities are flexible and easily controllable using small amounts of energy [13]. These features create situations where tensegrity structures are particularly attractive for active and deployable structures.

As a special type of prestressed pin-jointed framework, tensegrity structures are composed of axially loaded elements and this provides opportunities for actuation and deployment through changing element lengths. Length changes can be made to struts and cables through various actuation strategies. Strut-based actuation, employing telescopic members, has already been used in active tensegrity control applications. Fest et al. [14] experimentally explored shape control of a five-module large-scale active tensegrity structure. The actuation strategy was based on controlling the self-stress state of the structure through small movements of ten telescopic struts. This actuation was also used for self-diagnosis, self-repair and vibration control [1, 15]. Kanchanasaratool and Williamson [16] used actuated struts to perform feedback shape control for a simple tensegrity module. Hanaor [17] studied deployment of a simplex-based tensegrity grid using telescopic struts. Tibert and Pellegrino [18] numerically and experimentally investigated use of telescopic struts for the deployment of tensegrity reflectors. Generally, strut-based actuation becomes difficult to implement under conditions where internal forces are substantial, and required changes in shape are large. Furthermore, when strut-actuation is used for deployment, the structure may have no stiffness until it is fully deployed.

Cable-based actuation has been investigated in many research projects involving active and deployable structures. Bouderbala and Motro [19] studied folding of octahedron assemblies and showed that cable-mode folding was less complex than strut-mode, although the latter produced a more compact package. Djouadi et al. [20] developed a cable-control strategy for vibration damping of a tensegrity structure. Sultan and Skelton [5] proposed a tendon-control deployment strategy for tensegrity structures. Actuation is conducted in such way that the structure goes throughout successive equilibrium configurations. Wroldsen et al [6] investigated shape control of a tensegrity prism where actuation is performed by changing cable rest-lengths. Pinaud et al [21, 22] implemented tendon control deployment of a small-scale tensegrity boom composed of two tensegrity modules and studied asymmetrical reconfigurations during deployment. Smaili and Motro [23] investigated folding of tensegrity systems by activating finite mechanisms. A cable-control strategy is applied to a double-layer tensegrity grid. The proposed strategy is then extended to the folding of curved tensegrity grids [4]. Similarly, Sultan [24] presented a shape-control strategy for tensegrity structures in which the motion is controlled through infinitesimal mechanisms directions.

Most research studies of deployment of tensegrity structures showed that cable-actuation strategy directs tensegrity structures to maintain stiffness as they move from one equilibrium position to another. There are, however, a few disadvantages with this approach. Tibert and Pellegrino [25] argued that controlling cables is complicated, because of all the additional mechanical devices that are necessary. The deficiency of having to control too many cable elements can be overcome by connecting several cables together and using only one motor to control them [5]. This suggests that groups of individual active cable elements could be combined into continuous active cables. A single continuous cable can slide over multiple nodes through frictionless pulleys. This strategy has the advantage that fewer actuators are necessary for control. However, using continuous cables significantly changes the mechanics of classical tensegrity structures. Specifically the number of self-stress states can decrease and the mechanisms can increase [26]. This leads to significant challenges for structural analysis, control and actuation.

Finite-element formulations for sliding cable elements have been developed for modeling of suspension systems [27-30] and fabric structures [31]. Kwan and Pellegrino [32] proposed a matrix formulation for an active-cable macro-element consisting of two or more straight segments. The authors derived the equilibrium and flexibility matrices of active cable elements and pantographic elements that have been used in deployable structures. Chen et al [33] presented a formulation of multi-node sliding cable element for the analysis of Suspen-Dome structures. Genovese [34] investigated an approach to form-finding and analysis of tensegrity structures with sliding cables. The complete formulation of such systems was provided by Moored and Bart Smith [35]. Moored and Bart-Smith [35] formulated the potential energy, equilibrium equations and stiffness matrix for tensegrity structures with continuous cables. The equilibrium equations of a tensegrity structure are non linear. Analysis can thus be carried out in an iterative manner through use of the transient stiffness method. Matrix methods generally require iterative assembling and inversion of large stiffness matrices. As a vector-based method, the dynamic relaxation method (DR) does not require such complexity. This method introduced by Otter [36] and Day [37] in the mid-1960s is particularly attractive for modeling nonlinear structural behaviour. DR is an explicit iterative method for the static solution of structural-mechanics problems [38]. When the DR method is used, the static problem is transformed into a pseudo-dynamic one by introducing fictitious inertia and damping terms in the equation of motion. DR traces the motion of each node of a structure until, due to artificial damping, the structure comes to rest in static equilibrium. One of the advantages of this method is that global stiffness matrix is not needed and hence the method is particularly suitable for problems with material and geometrical nonlinearities. DR has been used by many researchers to solve a wide variety of engineering problems [39-45]. Furthermore, Barnes [46, 47] showed that DR is particularly efficient for form finding and analysis of tension structures. Hundreds, perhaps thousands of structures such as cable-stayed bridges and large tent structures have been designed and then analyzed using DR. For a tensegrity structure with continuous cables, the uncoupled nature of the DR process makes it particularly straightforward to implement [44].

In this paper, a modified dynamic relaxation algorithm applicable to the analysis of tensegrity structures with continuous cables is proposed. In the following section, characteristics and modeling of this particular class of tensegrity structures are first investigated. The subsequent section introduces the modified dynamic relaxation method. Governing equations, formulation of residuals forces, masses and damping strategy are described. The modified DR algorithm is described in detail. Numerical results are presented in Section 4. The algorithm is validated by simulating load response, actuation and deployment of two active tensegrity structures. Results are compared with those obtained employing a stiffness-based algorithm to show effectiveness of the proposed methodology.

2. Characteristics and modeling of clustered tensegrity structures

2.1 Basic assumptions

Moored and Bart-Smith [35] proposed the term "*clustered tensegrity*" to denote a particular class of tensegrity structures having sliding or continuous cables. This terminology is adopted in this paper. Since the use of the term "*clustering*" can be confusing, the definition of a clustered tensegrity is emphasized here. A clustered tensegrity is defined to be a tensegrity structure where at least two cable elements are grouped together to become a single element. "*Clustering*" can be achieved by having a cable sliding around a pulley pinned to a node thereby replacing two or more cables in the structure with one. Each group of individual cables that are combined into one continuous cable is then called a "*cable-element cluster*". Furthermore, actuation strategy employing active cable clusters is denoted as "*clustered actuation*". In addition to these definitions, the following modeling assumptions are made:

- Tensegrity members are connected by pin-joints.
- External loads are applied at nodes.
- Self-weight is transferred to nodes as point loads. Consequently, non-axial stresses in the tensegrity members are neglected.
- For clustered elements, cable groups are assumed to run over small frictionless pulleys attached to joints.
- Actuation is performed through small and slow steps such that inertia effects can be neglected when the structure is in motion.

2.2 Equilibrium equations of clustered tensegrity structures

As stated in the modeling assumptions, actuation is conducted in such way that the structure goes through successive equilibrium configurations. Friction and dynamic effects are not taken into account in this study. Only static behavior of clustered tensegrity structures is studied in this paper. Moored and Bart-Smith [35] showed that clustering significantly changes the mechanics of tensegrity structures. However, the governing equations for a clustered tensegrity structure are related to those of an equivalent classic tensegrity (without clustered elements). This property is exploited in this paper for the analysis of clustered tensegrity structures using a modified dynamic relaxation algorithm. The relationship between equilibrium equations of a clustered tensegrity structure and those of an equivalent classic tensegrity are explained in the next paragraph through a simple example.

Consider the three-element structure shown in Figure 1(a). The unconstrained reference node 1 is connected to nodes 2, 3 and 4 by members e_{12}, e_{13} and e_{14}, respectively. All three elements are supposed to be tensioned.

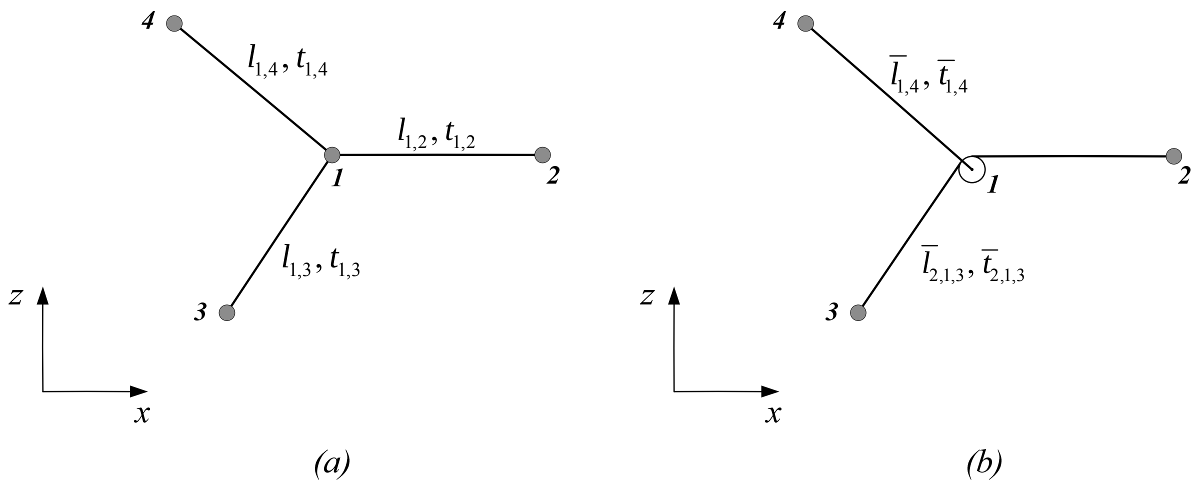

Figure 1. A three-element structure and the equivalent configuration with one continuous cable.

The equilibrium equations of node 1 are given by Eq.(1), where each member $e_{A,B}$ has an internal force $t_{A,B}$ and a length $l_{A,B}$. f_1 is an external force applied to node 1.

$$\begin{aligned}
(x_1-x_2)t_{1,2}/l_{1,2} \quad + \quad (x_1-x_3)t_{1,3}/l_{1,3} \quad + \quad (x_1-x_4)t_{1,4}/l_{1,4} &= f_{1,x} \\
(y_1-y_2)t_{1,2}/l_{1,2} \quad + \quad (y_1-y_3)t_{1,3}/l_{1,3} \quad + \quad (y_1-y_4)t_{1,4}/l_{1,4} &= f_{1,y} \\
(z_1-z_2)t_{1,2}/l_{1,2} \quad + \quad (z_1-z_3)t_{1,3}/l_{1,3} \quad + \quad (z_1-z_4)t_{1,4}/l_{1,4} &= f_{1,z}
\end{aligned} \qquad \text{[Eq.1]}$$

The matrix form of Eq.(1) relates an equilibrium matrix **A,** an internal force vector **t** and an external force vector **f** :

$$\mathbf{At} = \mathbf{f} \qquad \text{[Eq.2]}$$

Consider now the clustered two-element structure shown in Figure 1(b). For this configuration, elements $e_{1,2}$ and $e_{1,3}$ are replaced by a single element $\bar{e}_{213}$ that is assumed to run over a small frictionless pulley connected to node 1. The structure with one continuous cable (Figure 1(b)) is thus composed of two elements $\bar{e}_{213}$ and $\bar{e}_{14}$. For simplicity we will denote the two-element structure with continuous cable as the clustered structure and the equivalent systems without continuous elements as the classic structure.

The characteristics of the clustered structure set of elements, $\bar{e}$, can be easily written in terms of the characteristics of the classic structure set of elements, *e*. For instance, element lengths of the clustered structure can be related to element lengths of the equivalent classic structure by Eq.(3).

$$\begin{aligned} \bar{l}_{2,1,3} &= l_{1,2} + l_{1,3} \\ \bar{l}_{1,4} &= l_{1,4} \end{aligned} \qquad \text{[Eq.3]}$$

Eq.(3) can be written in matrix form, where the element lengths of the clustered structure are related to element lengths of the classic structure through a transformation matrix composed of 0/1 elements (Eq.(4)).

$$\begin{Bmatrix} \bar{l}_{2,1,3} \\ \bar{l}_{1,4} \end{Bmatrix} = \begin{bmatrix} 1 & 1 & 0 \\ 0 & 0 & 1 \end{bmatrix} \begin{Bmatrix} l_{1,2} \\ l_{1,3} \\ l_{1,4} \end{Bmatrix} \qquad \text{[Eq.4]}$$

Moored and Bart-Smith [35] called this transformation matrix the *clustering matrix*, $\mathbf{S} \in \mathbb{R}^{\bar{e} \times e}$ and showed that this matrix can be defined as follow:

$$S_{ij} = \begin{cases} 1, & \textit{if the classic element } e_j \textit{ is part} \\ & \textit{of element cluster } \bar{e}_i, \\ 0, & \textit{otherwise.} \end{cases} \qquad \text{[Eq.5]}$$

Through the clustering matrix **S**, the vector of element lengths of the classic structure, **l**, is transformed into a reduced set of element lengths of the clustered structure, $\bar{\mathbf{l}}$.

$$\bar{\mathbf{l}} = \mathbf{S}\mathbf{l} \qquad \text{[Eq.6]}$$

Equivalently, rest lengths of the clustered structure elements may be defined in the same way.

$$\bar{\mathbf{l}}_{\mathbf{0}} = \mathbf{S}\mathbf{l}_{\mathbf{0}} \qquad \text{[Eq.7]}$$

With the assumption that all element clusters run over frictionless pulleys, each continuous cable in the clustered structure can be assumed as a string of cable sub-elements all carrying the same tensile force. The vector of internal forces of the clustered structure elements can thus be related to the vector of internal forces of the classic structure elements through transposition of the clustering matrix.

$$\mathbf{t} = \mathbf{S}^{\mathbf{T}}\bar{\mathbf{t}} \qquad \text{[Eq.8]}$$

As for the classic structure, equilibrium equations of the clustered structure are based on nodal equilibrium under the action of the external load components of vector **f** and the internal force components of vector **t**. Substituting the vector of internal forces **t** by the product $\mathbf{S}^{\mathbf{T}}\overline{\mathbf{t}}$ yields the equilibrium equations for the clustered structure (Eq.(9)).

$$\mathbf{A}\,\mathbf{S}^{\mathbf{T}}\overline{\mathbf{t}} = \mathbf{f} \qquad \text{[Eq.9]}$$

Moored and Bart-Smith [35] obtained the same expression for the equilibrium condition of a general clustered tensegrity using more fundamental energy approach. They also derived the stiffness matrix by deriving equilibrium equations. Analysis of clustered tensegrities can thus be achieved in an iterative manner using transient stiffness method. We will show in the next section that, based on the formulation of the equilibrium equations, a modified dynamic relaxation algorithm can efficiently be used for analysis of clustered tensegrities.

3. Formulation of the modified dynamic relaxation method

The DR is based on the fact that the static solution of both linear and non linear structures subject to load may be regarded as the limiting equilibrium state of damped structural vibrations. Hence, when the DR method is used to solve a static problem, the static problem is transformed into a pseudo-dynamic one by introducing fictitious inertia and damping terms in the equation of motion. Since the DR method is an explicit finite difference solver, a time marching procedure is used to solve the equations of motion. Thus, DR traces the motion of each node of a structure until, due to artificial damping, the structure comes to rest in a stable static equilibrium. Note that only internal and external forces represent the physical problem, mass terms and damping strategy do not need to represent the physical structure. However, damping, mass and time increments should be selected so that the transient response is rapidly attenuated leaving the static solution for the applied load. Before proposing modifications to the DR algorithm, an overview of the basic governing equations of this method is given to provide the necessary background.

3.1 Governing equations

The DR method follows from augmenting static equilibrium equations (Eq.10) by including inertial and damping terms (Eq.11):

$$\mathbf{F}_{int}(\mathbf{u}) = \mathbf{F}_{ext} \qquad \text{[Eq.10]}$$

$$\left\{\mathbf{M}\,\dot{\mathbf{v}} + \mathbf{C}\,\mathbf{v}\right\} + \mathbf{F}_{int}(\mathbf{u}) = \mathbf{F}_{ext} \qquad \text{[Eq.11]}$$

In Equations 10 and 11, **u** and **v** are the vectors of nodal displacements and velocities, **M** and **C** are the mass and damping matrix, $\mathbf{F}_{int}$ is the vector of internal forces and $\mathbf{F}_{ext}$ is the vector of external forces. Introducing the residual force vector **R** as the difference between external and internal forces at any time *t*, Eq.(11) becomes

$$\mathbf{M}\,\dot{\mathbf{v}}^{t} + \mathbf{C}\,\mathbf{v}^{t} = \mathbf{R}^{t} \qquad \text{[Eq.12]}$$

Due to damping, nodal velocities and accelerations decay to zero as the solution is approached. The transient response is attenuated leaving the steady state solution for the applied load. The static equilibrium is thus attained and the out-of-balance or residual forces come to zero.

To obtain the DR basic equations, the following central difference approximations are used for temporal derivatives:

$$\mathbf{v}^{t} = \frac{\mathbf{v}^{t+\Delta t/2} + \mathbf{v}^{t-\Delta t/2}}{2}, \quad \dot{\mathbf{v}}^{t} = \frac{\mathbf{v}^{t+\Delta t/2} - \mathbf{v}^{t-\Delta t/2}}{\Delta t} \qquad \text{[Eq.13]}$$

Using these approximations, Equation (11) can be re-arranged to give the recurrence equations for nodal velocities where subscript *i,x* refers to the i^{th} node and direction *x* (respectively, for directions *y* and *z*):

$$v_{i,x}^{t+\Delta t/2} = v_{i,x}^{t-\Delta t/2}\left(\frac{M_{i,x}/\Delta t - C_{i,x}/2}{M_{i,x}/\Delta t + C_{i,x}/2}\right) + R_{i,x}^{t}\left(\frac{1}{M_{i,x}/\Delta t + C_{i,x}/2}\right) \qquad \text{[Eq.14]}$$

The velocities are then used to predict displacements at time ($t + \Delta t$):

$$u_{i,x}^{t+\Delta t} = u_{i,x}^{t} + \Delta t \,.\, v_{i,x}^{t+\Delta t/2} \qquad \text{[Eq.15]}$$

The iterative process of DR method consists of a repetitive use of Eq.(14) and (15). The process continues until the residual forces are close to zero. The values of masses M and damping C have to be chosen to ensure that the recurrence scheme converge to the static equilibrium [38]. Generally, a diagonal mass matrix is used along with a mass proportional damping matrix. This strategy involves the determination of a critical viscous damping coefficient. An alternative damping approach is the use of kinetic damping. This approach is adopted in this study and is described in detail in the following sections.

3.2 Residual forces of clustered elements

The modification introduced to DR in order to adapt it to the analysis of clustered tensegrities is concerned with the calculation of the residual forces. Since clustering considerably affects the distribution of internal forces in a clustered structure, residual forces are affected. The entire procedure for residual force calculation is listed in Table 1.

At each time step *t*, Eq.(15) is used to determine current node coordinates of the structure. The new member-length vector is thus easily determined. Current clustered tensegrity element lengths can be calculated using Eq.(6). Subsequently, current internal forces in the *m*th-member of the clustered tensegrity may be determined as follows:

$$\bar{t}_m^t = \frac{\bar{E}_m \bar{A}_m}{\bar{l}_{0,m}} \left(\bar{l}_m^t - \bar{l}_{0,m} \right) + \bar{t}_m^0 \quad \text{[Eq.16]}$$

where $\bar{l}_{0,m}$ and $\bar{l}_m^{t+\Delta t}$ are rest and current length of clustered member *m*. $\bar{E}_m$, $\bar{A}_m$ and $\bar{t}_m^0$ are Young modulus, cross-section area and initial prestress of clustered member *m*.

Once the vector of internal forces in the clustered tensegrity elements ($\bar{\mathbf{t}}$) is determined, the vector of internal forces in the tensegrity members ($\mathbf{t}$) can be computed employing Eq.(8). The residual forces can thus be calculated. For any node *i*, the residual force in *x*-direction $R_{i,x}$ is calculated as the sum of the external force $f_{ext,i,x}$ and the *x*-component of the resultant force induced by the contributions of the *N* members meeting at node *i*. Eq.(17) gives the expression of the *x*-component of the residual force at node *i* where t_m^t and l_m^t are tension and length of member *m* connecting node *i* to node *j*. Similar equations may be written for the *y* and *z* coordinate directions.

$$R_{i,x}^t = f_{ext,i,x} + \sum_{m=1}^{N} \frac{t_m^t}{l_m^t} \left(x_{j,m}^t - x_{i,m}^t \right) \quad \text{[Eq.17]}$$

Table 1: Algorithm for residual force calculation

I. inputs	At any time step, *t*: Current nodal coordinates Clustering matrix, $\mathbf{S}$ Clustered-element properties: Young modulus, $\bar{E}_m$; cross-section area, $\bar{A}_m$; rest-length, $\bar{l}_{0,m}$ and prestress, $\bar{t}_m^0$
II. computation	(1) Calculation of element length vector, $\mathbf{l}$ (2) Calculation of the vector of clustered-element lengths $\bar{\mathbf{l}} = \mathbf{S}\mathbf{l}$ (3) Calculation of clustered-element internal forces, $\bar{t}_m^t = \frac{\bar{E}_m \bar{A}_m}{\bar{l}_{0,m}} \left(\bar{l}_m^t - \bar{l}_{0,m} \right) + \bar{t}_m^0$ (4) Calculation of element internal forces, $\mathbf{t} = \mathbf{S}^{\mathbf{T}} \bar{\mathbf{t}}$ (5) If (cable element and compression force): $t_m = 0$ (6) Calculation of residual force, for each node *i* and direction *x* (respectively, for *y* and *z*) $R_{i,x}^t = f_{ext,i,x} + \sum_{m=1}^{N} \frac{t_m^t}{l_m^t} \left(x_{j,m}^t - x_{i,m}^t \right)$ (7) Reset the residuals of all fixed or partially constrained nodes to zero

3.3 Fictitious masses and kinetic damping

In the DR method the mass matrix, damping and time increment should be defined in such way that the stability and convergence of the iterative procedure is guaranteed [48]. Generally, if the time interval is too large or the masses too small, then instability of the iteration may occur. The analysis will thus not converge to an equilibrium position. Furthermore, damping is a key parameter in the DR method. Overdamping or underdamping impedes the convergences to a stable equilibrium state [49]. Various approaches to the selection of the foregoing parameters have been published in the literature [38, 48-51]. The most common method of determining mass terms is to use Gerschgörin's theorem. This theorem gives the following general expression that must be satisfied in order to guarantee the stability of the iterations [38]:

$$M_i \geq \frac{1}{4}\Delta t^2 \sum_j \left| k_{i,j} \right| \qquad \text{[Eq.18]}$$

where $k_{i,j}$ are the elements of the tangent stiffness matrix.

Barnes [47] addressed form-finding and analysis of tension structures and studied stability and setting of mass components. According to Barnes [47], the mass at any node *i* should be set to comply with Eq.(19) in order to guarantee the stability of the iterations for an arbitrarily chosen value of the time increment Δt.

$$M_{i,x} = \left(\frac{\Delta t}{0.5} \right)^2 \frac{k_{i,x}}{2} \qquad \text{[Eq.19]}$$

For each node of the structure, the direct stiffness k_i is calculated by summing up contributions of all members meeting at node *i*. For tensioned members, the main stiffness component should account for both elastic and geometric stiffness. A stiffness term is thus assigned to each coordinate direction (Eq.(20)).

$$k_{i,x} = \sum_{m=1}^{N} \left(\frac{E_m A_m}{l_{0,m}} + \frac{t_m}{l_m} \right) \left(\frac{x_{j,m} - x_{i,m}}{l_m} \right)^2 \qquad \text{[Eq.20]}$$

Similar equations may be written for $k_{i,y}$ and $k_{i,z}$ for node stiffness in the *y* and *z* coordinate directions. Three nodal mass components are thus assigned to each node resulting in a 3×3 block diagonal nodal mass matrix. It should be pointed out that the geometric stiffness (t_m / l_m) is set to zero for members in compression and slack cables. On the other hand, boundary conditions may be imposed by assigning large masses to fixed joints.

Kinetic damping is adopted in this work. In contrast with viscous damping, which assumes that connection between the nodes has a viscous force component, kinetic damping is artificial damping with no real effect. Employed successfully by many authors, kinetic damping has been found to be stable and rapidly convergent when dealing with large displacements [47, 50, 52]. When kinetic damping is employed, the viscous damping coefficients in Eq.(14) are no longer needed. As dynamic relaxation iterations proceeds, the kinetic energy of the undamped structure is calculated. When a kinetic peak is detected, all nodal velocities are set to zero and the current coordinates are taken as starting values for the next cycle of iterations. The analysis continues, progressively eliminating the kinetic energy from various modes of vibration until the required degree of convergence is obtained. Tracing kinetic energy is based on the fact that, in simple harmonic motion, maximum kinetic energy is achieved in a configuration that corresponds to static equilibrium position with minimum potential energy. The adoption of kinetic damping thus eliminates the need to compute optimized viscous damping coefficients and offers a substantial reduction in the number of iterations required to find a solution. Furthermore, this strategy can efficiently accommodate geometrical inaccuracies and stiffness modifications [44].

3.4 DR algorithm

The complete algorithm for the DR method used for a clustered tensegrity structure is presented in Table 2. When the process starts, residual forces and kinetic energy are set to zero. Nodal velocities are initialized using Eq.(21).

$$v_{i,x}^{\Delta t/2} = \frac{\Delta t}{2M_{i,x}} R_{i,x}^{0} \qquad \text{[Eq.21]}$$

This gives effectively $v_{i,x}^{\Delta t/2} = -v_{i,x}^{-\Delta t/2}$, i.e. $v_{i,x} = 0$ at time zero. Velocities are similarly reset to zero after each energy peak (step (4.4) in Table 2). As DR iterations proceeds, the kinetic energy of the structure is monitored. It can be deduced that an energy peak has occurred when the current value of kinetic energy is smaller than the value of the previous iteration. Since the iterative process is punctuated by discrete time intervals Δt, the point at which the kinetic energy reached a maximum value is not precisely determined and a small correction of nodal coordinates is thus needed (step (4.1) in Table 2). At this point, nodal velocities are reset to zero and the corrected coordinate values are taken as starting values for the next cycle of iterations [47, 53]. The iterative process continues until static equilibrium is attained when the norm of the vector of residual forces goes below a fixed precision value.

Table 2: The DR algorithm for clustered tensegrity analysis

I. Initialize

$t = 0, \quad u^0 = 0, \quad KE = 0, \quad R_{tol} = 10^{-5}, \quad \Delta t = 0.01$

calculate clustering matrix and clustered-member properties

calculate initial residual forces, $R^0_{i,x}$ (Table 1)

calculate nodal masses, $M_{i,x}$ (Equations (19) and (20))

calculate initial velocities, $v^{\Delta t/2}_{i,x}$ (Eq.(21))

II. Iteration process

(1) velocity update

$$v^{t+\Delta t/2}_{i,x} = v^{t-\Delta t/2}_{i,x} + \frac{\Delta t}{M_{i,x}} R^t_{i,x}$$

(2) update displacement and nodal coordinate

$$u^{t+\Delta t}_{i,x} = u^{t-\Delta t}_{i,x} + \Delta t\, v^{t+\Delta t/2}_{i,x}$$

$$x^{t+\Delta t}_i = x^t_i + u^{t+\Delta t}_{i,x}$$

(3) calculate current kinetic energy

$$KE^{t+\Delta t} = \tfrac{1}{2} \sum_{i,x} M_{i,x} \left(v^{t+\Delta t}_{i,x} \right)^2$$

(4) if $KE^{t+\Delta t} \le KE^t$: energy peak detected otherwise go to step (5)

(4.1) nodal coordinate correction

$$x^{t+\Delta t}_i = x^{t+\Delta t}_i - \tfrac{3}{2} \Delta t\, v^{t+\Delta t}_{i,x} + \tfrac{1}{2} \Delta t^2 \frac{R^t_{i,x}}{M_{i,x}}$$

(4.2) recalculate residual forces, $R^t_{i,x}$ (Table 1)

(4.3) check convergence:

if $\left\| \mathbf{R}^t \right\| \le R_{tol}$ go to step (8); otherwise continue

(4.4) reset velocities to zero

$$v^{t+\Delta t/2}_{i,x} = \frac{\Delta t}{2M^t_{i,x}} R^t_{i,x}$$

(4.5) reset kinetic energy to zero : $KE^{t+\Delta t} = 0$

(5) update residual forces, $R^{t+\Delta t}_{i,x}$ (Table 1)

(6) update nodal masses, (Equations (19) and (20))

(7) $t = t + \Delta t$ and go to step (1)

(8) print the results and stop;

4. Numerical examples

In this section, two numerical examples are presented and discussed in order to show the efficiency of the proposed DR procedure in predicting the non linear response of clustered tensegrity structures. A computer program is developed based on the above-mentioned algorithm (Table 2). For the verification purpose transient stiffness method, based on Moored and Bart-smith formulation [35], is also programmed. The efficiency of the proposed DR algorithm is first demonstrated through analysis of a clustered tensegrity beam. Both actuation response and load response of the clustered tensegrity beam are investigated. Deployment through clustered actuation is also simulated numerically. A deployable quadruplex-based structure is studied. For all numerical cases, computations were stopped when the norm of the vector of residual forces was below 10^{-4}.

4.1 Tensegrity beam

The performance of the proposed modified DR algorithm is demonstrated using the topology of a clustered tensegrity structure studied by Moored and Bart-Smith [35]. The structure is a tensegrity beam composed of an assembly of three prismatic modules commonly known as quadruplex modules.

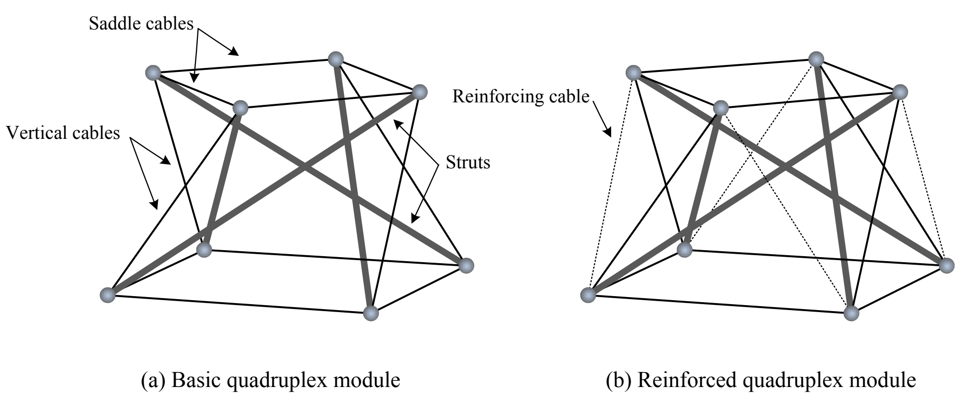

Figure 2. Quadruplex module

The quadruplex unit shown in Fig.2 (a) comprises four struts held together in space by 12 cables. When only rigid-body movements are blocked, this tensegrity unit has a unique state of self-stress and three infinitesimal mechanisms. The module can be reinforced by adding four reinforcing cables which remove mechanism modes from the structure (Fig.2 (b)).

Three reinforced modules are connected together with no bar-to-bar connections, forming a class 1 tensegrity structure. A perspective view of the tensegrity beam is given in Fig. 3 where grayed lines denote bars and thin lines denote cables. Three of the end nodes of the structure (nodes 1, 3 and 6) are pinned forming a cantilever beam. Ten cable elements of the top surface and ten cable elements of the bottom surface of the structure are grouped into four cable-element clusters. In

Fig.4, clustered elements are shown in dashed lines in a top view of the tensegrity beam. Each cable cluster is attached to two end nodes and runs frictionnlessly through four intermediate nodes. Details of the four cable clusters are given in Table 3.

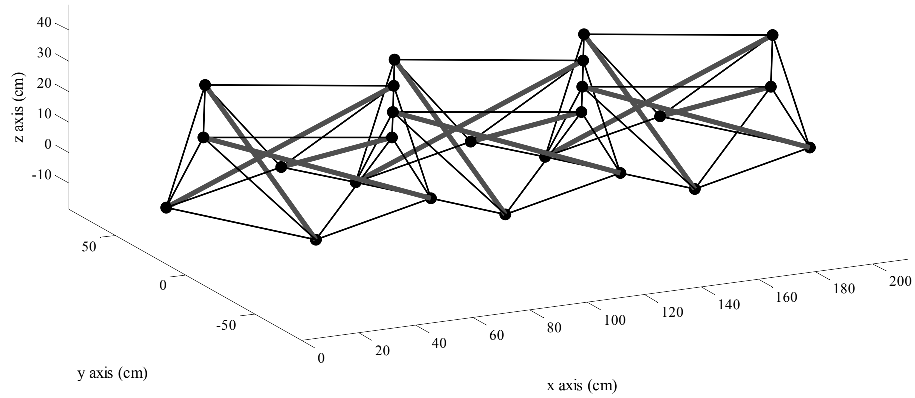

Figure 3. A perspective view of the tensegrity beam

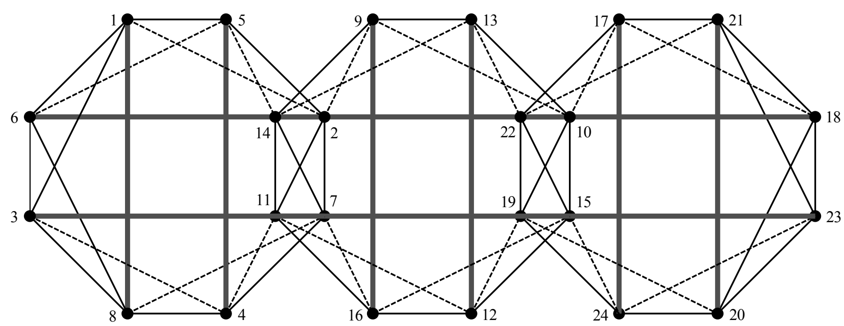

Figure 4. Clustered elements of the tensegrity beam

Table 3: Details about clustered cables

Cable	Position	End nodes	Intermediate nodes
1	Top surface	6 and 21	5, 14, 13 and 22
2	Top surface	8 and 23	7, 16, 15 and 24
3	Bottom surface	1 and 18	2, 9, 10 and 17
4	Bottom surface	3 and 20	4, 11, 12 and 19

The tensegrity beam used in this study has a length of 212cm, a width of 80cm and a height of 30cm. Struts are made of aluminum hollow tubes with a length of 85cm. Saddle, vertical and reinforcing cables have a length of 60, 48 and 40 cm, respectively. All cable members are made by stainless-steel. Detailed characteristics of used members are summarized in Table 4.

Table 4: Material characteristics for the tensegrity beam

Member	Material	Cross-section area (cm^2)	Young modulus (kN/cm^2)	Specific weight (kN/cm^3)

Struts	Aluminum	2.55	7000	2.7 10^{-5}
Cables	Stainless-steel	0.5026	11500	7.85 10^{-5}

Actuated bending deformation of the tensegrity beam is first studied. Bending deformation can be obtained through antagonist actuation of the of top and bottom cable clusters. Actuation is performed by changing the effective rest length of active cables. For example, a prescribed actuation stroke of 20% is defined as a change in the rest length of 20%. Prior to actuation, top cluster cables are contracted by 2% in order to introduce self-stress in the structure and counteract deflection induced by self-weight. The tensegrity beam is then actuated through modifying lengths of the four clustered cables. Top clusters are actuated with 10% contraction while the bottom clusters are expanded by 10%. Contraction and elongation of active clusters is made progressively in steps of 1%. Note that actuation is deliberately performed through small and slow steps such that inertia effects can be neglected when the structure is in motion. The actuation response obtained by the proposed DR method and transient stiffness method based on Moored and Bart-Smith formulation [35] are compared in Fig. 5. Displacements at the top node 18 of the beam are displayed with respect to the actuation ratio in active elements (Fig.5). It is observed that the result of the present study are in agreement with those obtained by Moored and Bart-Smith [35].

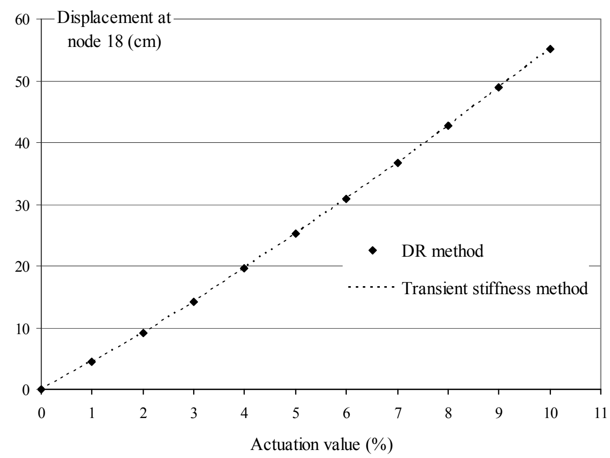

Figure 5. Actuation-response of the clustered tensegrity beam

When the top clusters have been actuated with 10% contraction while the bottom clusters have been expanded by 10%, this results in a 55cm tip deflection in the positive z-direction (Fig.6).

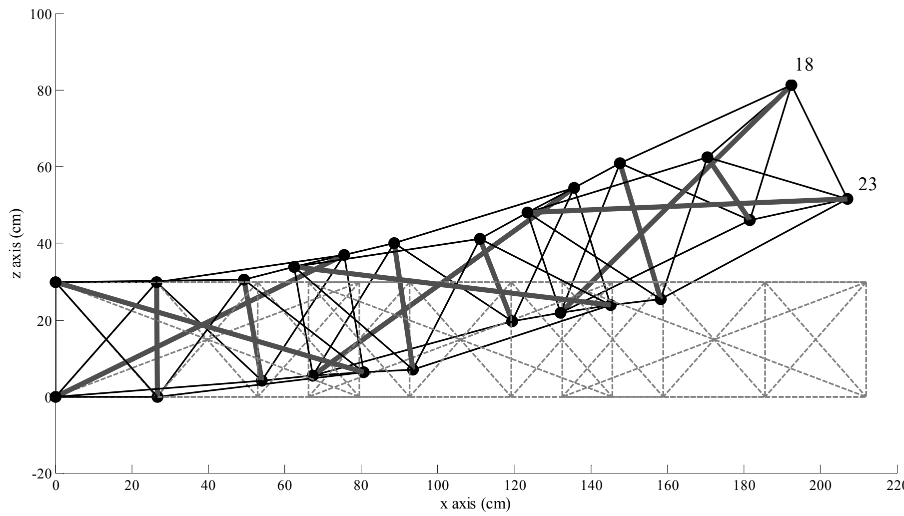

Figure 6. Deformed shape of the tensegrity beam due to 10% actuation of cable clusters

The efficiency of each method is studied in terms of the CPU time required for a solution. Results displayed in Table 5 indicate that for the DR method convergence is achieved in an average time of 1.10s. For the transient stiffness method, the average CPU time needed for convergence for the eleven runs is smaller (0.34s). The transient stiffness algorithm requires a fewer number of iterations than the DR algorithm. Furthermore, the number of iterations for the eleven runs of the two methods varies little.

Table 5: Efficiency comparison between DR and transient stiffness methods

Actuation ratio (%)	DR			Transient stiffness	
	Number of KE resets	Number of iterations	CPU time (s)	Number of iterations	CPU time (s)
0	36	11015	1.28	22	0.21
1	38	9916	1.23	27	0.25
2	39	11108	1.28	29	0.26
3	37	9796	1.13	31	0.28
4	40	8947	1.03	38	0.34
5	38	9240	1.08	48	0.44
6	42	9493	1.09	53	0.48
7	41	8343	0.97	37	0.33
8	39	9135	1.07	43	0.39
9	41	9012	1.05	37	0.33
10	42	7806	0.92	46	0.42

The efficiency of the two methods is further investigated through the study of their computational complexity [54]. Computational complexity is an algorithm-efficiency criterion independent of the computing technology employed. This criterion describes the efficiency of an algorithm according to factors such as task formulation and algorithm optimality that influence trends in execution time. This is achieved by expressing the relation between the relative influence of the size of input and the time taken for the algorithm to terminate.

The execution time of both DR and transient stiffness algorithms depends on the size and the degree of non linearity of the structure. The number of structure nodes (*n*) is used to describe the structure size. On the other hand, the number of iterations required for convergence is highly dependent on the degree of non linearity of the structure. In dynamic relaxation, the uncoupled vectorized process results in a linear complexity ($O(n)$). In the transient stiffness method, forming the tangent stiffness matrix and resolving the equilibrium system of equations are computationally intensive parts of the analysis. Employing a direct method to solve the equilibrium system of equations is at best of a $O(n^3)$ complexity.

The DR algorithm has a lower complexity compared with the transient stiffness algorithm. This implies that for a large structure, convergence is achieved with smaller execution time if the DR is employed rather than the transient stiffness method. For example, the execution time is evaluated on a class 2 tensegrity structure with 65 nodes and 245 members. The DR algorithm requires 0.54s to terminate; while the transient stiffness algorithm converges within 4.55s (both programs were executed on the same station). The DR converges faster for the class 2 tensegrity structure comparing to the 24 node class1 tensegrity structure. This discrepancy shows the influence of the degree of non linearity on the convergence rate of the DR method. The execution times obtained with the 65 node structure are used to estimate the execution time for a structure of 1'000 nodes.

Table 6: complexity analysis of the DR and transient stiffness algorithms

Algorithm	Complexity	Execution time for n = 65	Constant *c*	Estimated execution time for n = 1000
DR	$O(n)$	0.54 = c . 65	$8.3 \cdot 10^{-3}$	8.3 seconds
Transient stiffness	$O(n^3)$	$4.55 = c \,.\, 65^3$	$1.6 \cdot 10^{-5}$	4.6 hours

Table 6 shows the results for execution time estimations. The DR algorithm execution time estimated at approximately 8.3 seconds is much smaller than the execution time of the transient stiffness algorithm (around 4.6 hours). This example shows that the DR algorithm is more efficient for large structures. However, execution time evaluated for the two methods should be considered as estimations since convergence is also dependent on the degree of non linearity of the structure. Furthermore, further enhancement of both transient stiffness and DR methods may alter the values in the last column of Table 6 [48, 55]. However, trends will be the same.

Load-response of the clustered tensegrity beam is also investigated employing both DR and transient stiffness methods. The tensegrity beam is subjected to a vertical load applied at nodes 18 and 23. The load-displacement curves obtained by the proposed DR method and transient stiffness method based on Moored and Bart-Smith formulation [35] are compared in Fig. 7. It can be seen that the results predicted by the DR method are identical to those generated by the transient stiffness method.

Load-displacement curves of the clustered tensegrity beam obtained employing modified and unmodified dynamic relaxation are compared in Fig.8. This comparison reveals that predicted displacement are under estimated if the effect of cable clustering is not considered in the analysis. Results indicate that the clustered beam is about 55% more flexible than an equivalent configuration having discontinuous cables. This suggests that the nonlinear behaviour induced by large displacements is more accentuated in clustered tensegrity structures.

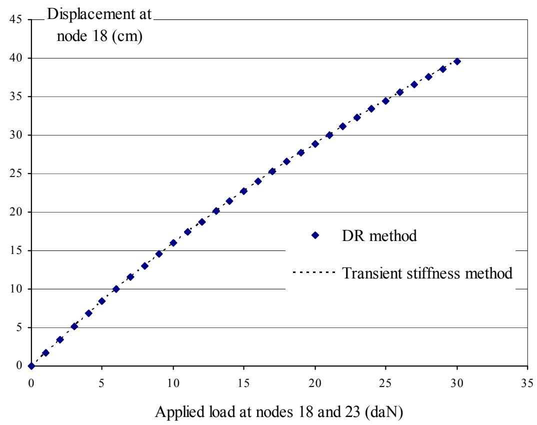

Figure 7. Load-displacement curves of the clustered tensegrity beam

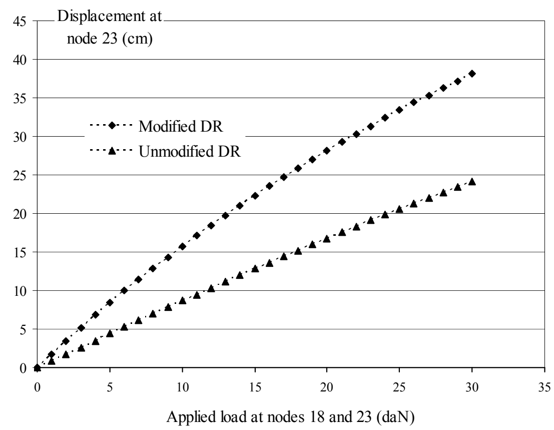

Figure 8. Load-displacement curves obtained employing modified and unmodified DR

4.2 Deployable two-module tensegrity structure

A two-module tensegrity structure is studied in this section. The structure is assembled from two identical qudruplex modules with four bar-to-bar connections (Fig.(9)). The structure has 8 struts held in space by 20 cables where the middle four saddle cables are shared by the two modules. Each two vertical cable elements running through top and bottom modules are grouped into one continuous cable running frictionnlessly through a pulley attached to the four nodes connecting the two modules.

Perspective and top views of the tensegrity structure are presented in Fig.(9) where dashed lines denotes the four cable clusters. For this study cable clusters are progressively actuated to achieve compacting and folding of the tensegrity structure. Compacting consists on unfolding the structure from its nominal configuration, corresponding to the operating conditions to an almost flat configuration. Deployment is achieved via opposite operation. Compacting and deployment of the tensegrity structure have to be performed such that all cables are maintained in tension and the bars do not touch each other.

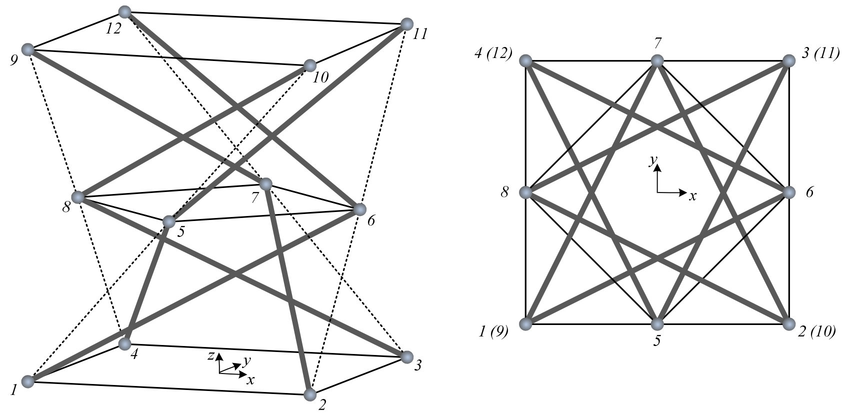

Figure 9. Perspective and top views of the two-module tensegrity structure

The tensegrity structure used in this example has a nominal height of 80cm. Struts are made of aluminum hollow tubes with a length of 100cm. The middle four saddle cables are replaced by four spring elements with a constant of 0.2kN/cm and a free length of 40cm. Top and bottom saddle cables has a rest length of 80cm. The four cable clusters have a rest length of 60cm. All cable members are made of stainless-steel. The characteristics of members are the same as for the tensegrity beam studied in the previous section (Table 4). Apart from self-weight, no external forces are taken into account. The four bottom nodes of the tensegrity structure are constrained. Node 1 is blocked in three translation directions; node 2 is blocked in y and z directions while nodes 3 and 4 are blocked in the z direction only.

Cable-based control is employed to fold and deploy the tensegrity structure. This is numerically simulated by shortening and elongating rest lengths of the four cable clusters. First, the structure is folded by progressively shortening active cables in steps of 0.5mm. The procedure is terminated when strut interference is detected. Bar collision is prevented through measuring the distance between struts at every step in the deployment process. The minimal accepted distance between two struts is taken to be 3cm. The reverse procedure is employed for deployment where the active cables are released progressively and the structure unfolds to its nominal configuration due to the energy stored in the spring elements during the compacting phase. Note that actuation is conducted in such way the structure goes through successive equilibrium configurations. In addition, cable-length adjustments are performed in slow and small steps to eliminate dynamic effects. Figure 10 shows three snapshots of the deployment process of the structure.

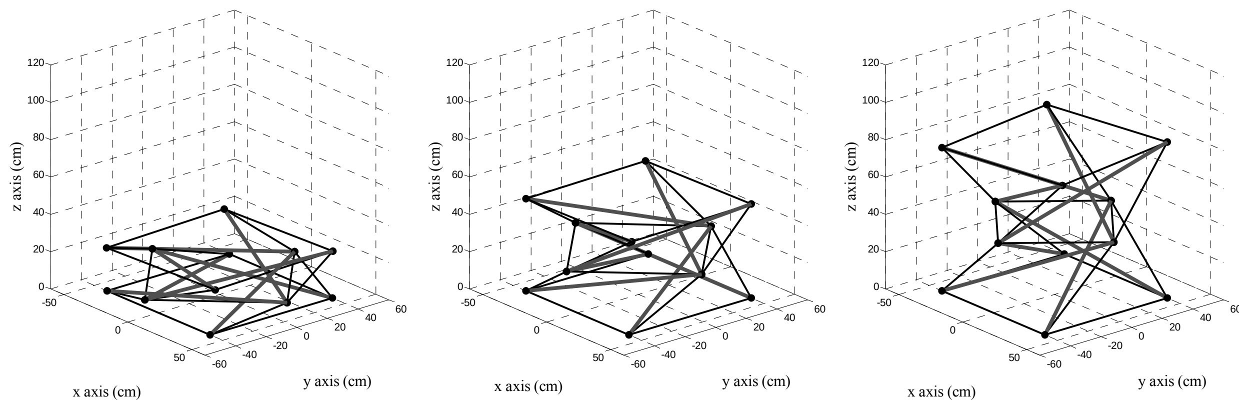

H = 26 cm **H = 50 cm** **H = 80 cm**

Figure 10. Snapshots of the deployment process of the two-stage tensegrity structure

The actuation response obtained by the proposed DR method and transient stiffness method based on Moored and Bart-Smith formulation [35] are compared in Fig. 11. The height of the module is displayed with respect to the length of active cable clusters (Fig.11). It is observed that the results obtained through the modified DR are in a good agreement with those obtained by the transient stiffness method.

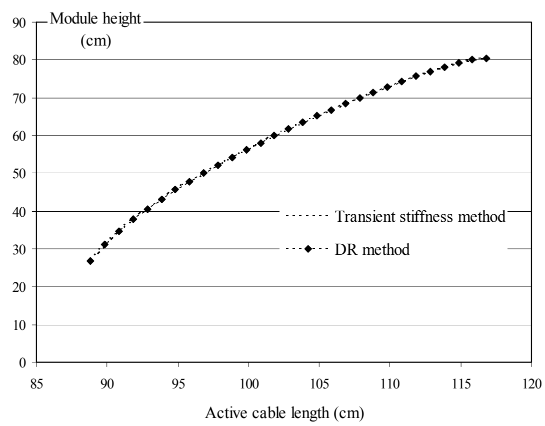

Figure 11. Actuation-response of the clustered tensegrity structure

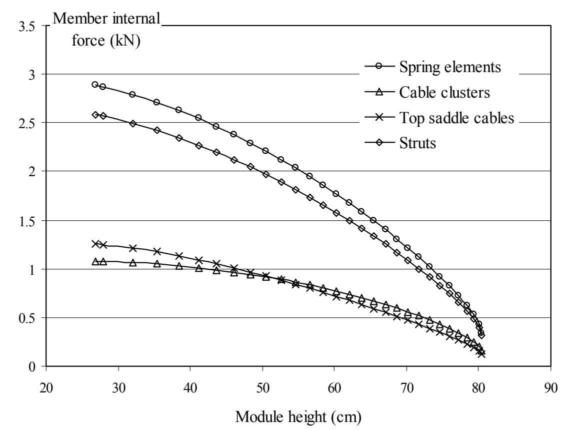

Figure 12. Internal force magnitudes in the tensegrity members during deployment

The deployment study shows that the tensegrity structure can be compacted to 32% of its nominal height. The compacted height decreases to 15% if the loads due to self-weight are not taken in account in the deployment analysis.

The evolution of the magnitude of the internal forces in the tensegrity members with respect to the structure height is displayed in Fig.12. It is shown that a relatively small level of self-stress is sufficient to ensure the stability of the tensegrity structure subjected only to its self-weight loads. In the compacted configuration, the level of self-stress in the structure increases. The elastic energy of the structure is mainly stored in spring elements. The comparison between the structure energy of the nominal and the compacted configurations gives insight into the energy needed for compacting process. Energy calculation show that for the clustered tensegrity, the energy needed for compacting is about 2.8kJ. For an equivalent configuration without continuous cables this energy is approximately in the same range (2.81kJ). Even if clustering did not reduce the energy needed for deployment, it considerably reduces actuation complexity, since clustering allows for a reduction in the number of actuators. In addition, for this configuration, actuators can be placed at the extremity of the structure. Technical difficulties related to embedded cable actuation are thus avoided.

5. Conclusions

Dynamic relaxation is an attractive static analysis method for tensile and tensegrity structures. The method is extended here to accommodate clustered tensegrity structures. In cable-based actuation of tensegrity structures, the deficiency of having to control too many cable elements can be overcome by connecting several cables. Continuous cables are thus used instead of discontinuous members. Clustered cables are assumed to run without friction through structural nodes. The concept of cable clustering is a scalable solution that can be employed for active structures that incorporate many active elements in order to reduce the number of actuators needed for active control and deployment. However, clustering cables significantly changes the mechanics of classical tensegrity structures and this leads to new challenges for structural analysis, control and actuation. This study shows that the uncoupled nature of the DR process makes it particularly attractive to apply to structures with clustered cable elements. The performance of the method compares favorably with the transient stiffness method. Two numerical examples show that the predictions of the modified DR method are in good agreement with those generated by the transient stiffness method. Finally, the DR method scales up to larger structures more efficiently due to lower computational complexity.

Acknowledgements

The authors would like to thank the Swiss National Science Foundation for supporting this work (FN Grant no 200020-121552/1). Keith W. Moored (University of Virginia) is thanked for discussion and for providing detailed data of the first example.

References

[1] Adam B, Smith IFC. Active tensegrity: A control framework for an adaptive civil-engineering structure. Computers & Structures. 2008;86(23-24):2215-23.

[2] Masic M, Skelton RE. Selection of prestress for optimal dynamic/control performance of tensegrity structures. International Journal of Solids and Structures. 2006;43(7-8):2110-25.

[3] Raja MG, Narayanan S. Active control of tensegrity structures under random excitation. Smart Materials and Structures. 2007;16:809-17.

[4] Smaili A, Motro R. Foldable/unfordable curved tensegrity systems by finite mechanism activation. Journal of the International Association for Shell and Spatial Structures. 2007;48(155):153-60.

[5] Sultan C, Skelton R. Deployment of tensegrity structures. International Journal of Solids and Structures. 2003;40(18):4637-57.
[6] Wroldsen AS, de Oliveira MC, Skelton RE. Modelling and control of non-minimal non-linear realisations of tensegrity systems. International Journal of Control. 2009;82:389-407.
[7] Juan SH, Mirats Tur JM. Tensegrity frameworks: Static analysis review. Mechanism and Machine Theory. 2008;43(7):859-81.
[8] Mirats Tur JM, Hernàndez Juan S. Tensegrity frameworks: Dynamic analysis review and open problems. Mechanism and Machine Theory. 2009;44(1):1-18.
[9] Skelton RE, de Oliveira MC. Tensegrity systems: Springer 2009.
[10] Skelton RE, Adhikari R, Pinaud JP, Waileung C, Helton JW. An introduction to the mechanics of tensegrity structures. *Proceedings of the 40th IEEE Conference on Decision and Control*. Orlando, FL, USA 2001:4254-9 vol.5.
[11] Wang BB. Free-Standing Tension Structures From Tensegrity Systems to Cable-Strut Systems Routledge, UK 2004.
[12] Bel Hadj Ali N, Rhode-Barbarigos L, Pascual Albi AA, Smith IFC. Design optimization and dynamic analysis of a tensegrity-based footbridge. Engineering Structures. 2010;In Press, Corrected Proof.
[13] de Jager B, Skelton RE. Input-output selection for planar tensegrity models. Control Systems Technology, IEEE Transactions on. 2005;13(5):778-85.
[14] Fest E, Shea K, Smith IFC. Active Tensegrity Structure. Journal of Structural Engineering. 2004;130(10):1454-65.
[15] Bel Hadj Ali N, Smith IFC. Dynamic behavior and vibration control of a tensegrity structure. International Journal of Solids and Structures. 2010;47(9):1285-96.
[16] Kanchanasaratool N, Williamson D. Modelling and control of class NSP tensegrity structures. International Journal of Control. 2002;75:123-39.
[17] Hanaor A. Double-layer tensegrity grids as deployable structures. International Journal of Space Structures. 1993;8:135-45.
[18] Tibert AG, Pellegrino S. Deployable Tensegrity Reflectors for Small Satellites. Journal of Spacecraft and Rockets. 2002;39(5):701-9.
[19] Bouderbala M, Motro R. Folding tensegrity systems. *IUTAM-IASS Symposium on Deployable Structures: Theory and Applications*. Cambridge, UK. 1998:27-36.
[20] Djouadi S, Motro R, Pons JC, Crosnier B. Active Control of Tensegrity Systems. Journal of Aerospace Engineering. 1998;11(2):37-44.
[21] Pinaud J-P, Solari S, Skelton RE. Deployment of a class 2 tensegrity boom. *Smart Structures and Materials 2004: Smart Structures and Integrated Systems* 2004:155-62.
[22] Pinaud J-P, Masic M, Skelton RE. Path planning for the deployment of tensegrity structures. *Smart Structures and Materials 2003: Modeling, Signal Processing, and Control* 2003:436-47.
[23] Smaili A, Motro R. Folding/unfolding of tensegrity systems by removal of self-stress. *IASS 2005 Symposium on Shell and Spatial Structures - Theory, Technique, Valuation, Maintenance*. Bucarest 2005:595-602.
[24] Sultan C. Tensegrity motion control using internal mechanisms. *Control Applications, (CCA) & Intelligent Control, (ISIC), 2009 IEEE* 2009:1276-81.
[25] Tibert AG, Pellegrino S. Deployable tensegrity masts. *44th AIAA/ASME/ASCE/AHS/ASC Structures, Structural Dynamics, and Materials Conference*. Norfolk, VA, USA 2003.

[26] Motro R, Raducanu V. Tensegrity Systems. International Journal of Space Structures. 2003;18:77-84.
[27] Aufaure M. A finite element of cable passing through a pulley. Computers & Structures. 1993;46(5):807-12.
[28] Zhou B, Accorsi ML, Leonard JW. Finite element formulation for modeling sliding cable elements. Computers & Structures. 2004;82(2-3):271-80.
[29] Pauletti RMO, Guirardi DM, Gouveia S. Modelling sliding cables and geodesic lines through dynamic relaxation. *IASS Symposium 2009, Evolution and trends in Design, Analysis and Construction of Shell and Spatial Structures*. Valencia 2009:2047-57.
[30] Hincz K. Nonlinear Analysis of Cable Net Structures Suspended From Arches with Block and Tackle Suspension System, Taking into Account the Friction of the Pulleys. International Journal of Space Structures. 2009;24(3):143-52.
[31] Pargana JB, Lloyd-Smith D, Izzuddin BA. Fully integrated design and analysis of Tensioned Fabric Structures: Finite elements and case studies. Engineering Structures. 2010;32(4):1054-68.
[32] Kwan ASK, Pellegrino S. Matrix formulation of macro-elements for deployable structures. Computers & Structures. 1994;50(2):237-54.
[33] Chen ZH, Wu YJ, Yin Y, Shan C. Formulation and application of multi-node sliding cable element for the analysis of Suspen-Dome structures. Finite Elements in Analysis and Design. 2010;46(9):743-50.
[34] Genovese D. Strutture tensegrity - Metodi di Analisi e Ricerca di Forma. *Dipartimento di Architettura, costruzioni, strutture*. Italy: Universita` Politecnica delle Marche 2008:82.
[35] Moored KW, Bart-Smith H. Investigation of clustered actuation in tensegrity structures. International Journal of Solids and Structures. 2009;46(17):3272-81.
[36] Otter JRH. Computations for prestressed concrete reactor pressure vessels using dynamic relaxation. Nuclear Structural Engineering. 1965;1(1):61-75.
[37] Day AS. An introduction to dynamic relaxation. The Engineer. 1965;219:218-21.
[38] Underwood P. Dynamic Relaxation. *Computational methods for transient analysis*. Belytschko, T. and Hughes, T.J.R. ed. Amsterdam Elsevier 1983:245-56.
[39] Douthe C, Baverel O. Design of nexorades or reciprocal frame systems with the dynamic relaxation method. Computers & Structures. 2009;87(21-22):1296-307.
[40] Dang HK, Meguid MA. Evaluating the performance of an explicit dynamic relaxation technique in analyzing non-linear geotechnical engineering problems. Computers and Geotechnics. 2009 2010/3//;37(1-2):125-31.
[41] Pan L, Metzger DR, Niewczas M. The Meshless Dynamic Relaxation Techniques for Simulating Atomic Structures of Materials. ASME Conference Proceedings. 2002;2002(46520):15-26.
[42] Salehi M, Aghaei H. Dynamic relaxation large deflection analysis of non-axisymmetric circular viscoelastic plates. Computers & Structures. 2005;83(23-24):1878-90.
[43] Zhang L, Maurin B, Motro R. Form-Finding of Nonregular Tensegrity Systems. Journal of Structural Engineering. 2006;132(9):1435-40.
[44] Wakefield DS. Engineering analysis of tension structures: theory and practice. Engineering Structures. 1999;21(8):680-90.

[45] Domer B, Fest E, Lalit V, Smith IFC. Combining Dynamic Relaxation Method with Artificial Neural Networks to Enhance Simulation of Tensegrity Structures. Journal of Structural Engineering. 2003;129(5):672-81.
[46] Barnes M. Form and stress engineering of tension structures. Structural Engineering Review. 1994;6(3-4):175-202.
[47] Barnes MR. Form Finding and Analysis of Tension Structures by Dynamic Relaxation. International Journal of Space Structures. 1999;14:89-104.
[48] Kadkhodayan M, Alamatian J, Turvey GJ. A new fictitious time for the dynamic relaxation (DXDR) method. International Journal for Numerical Methods in Engineering. 2008;74(6):996-1018.
[49] Metzger DR. Adaptive damping for dynamic relaxation problems with non-monotonic spectral response. International Journal for Numerical Methods in Engineering. 2003;56(1):57-80.
[50] Papadrakakis M. A method for the automatic evaluation of the dynamic relaxation parameters. Computer Methods in Applied Mechanics and Engineering. 1981;25(1):35-48.
[51] Rezaiee-pajand M, Alamatian J. The dynamic relaxation method using new formulation for fictitious mass and damping. Structural Engineering and Mechanics. 2010;34(1):109-33.
[52] Topping BHV, Khan AI. Parallel computation schemes for dynamic relaxation. Engineering Computations. 1994;11(6):513-48.
[53] Lewis WJ. Tension Structures: Form and Behaviour. London: Thomas Telford 2003.
[54] Raphael B, Smith IFC. Fundamentals of Computer Aided Engineering: John Wiley 2003.
[55] Yang Y-B, Yau J-D, Leu L-J. Recent developments in geometrically nonlinear and postbuckling analysis of framed structures. Applied Mechanics Reviews. 2003;56(4):431-49.